

Supporting Information

***In vivo* Biosynthesis of Tyrosine Analogs and their Concurrent Incorporation in a Residue-specific Manner for Enzyme Engineering**

Yumi Won,^{1#} Hyunwoo Jeon,^{1#} Amol D. Pagar,¹ Mahesh D. Patil,¹ Saravanan P. Nadarajan,¹ Dillon T. Flood,² Philip E. Dawson² and Hyungdon Yun^{1*}

¹ Department of Systems Biotechnology, Konkuk University, 120 Neungdong-ro, Gwangjin-gu, Seoul, 05029, Korea.

² Department of Chemistry, The Scripps Research Institute, 10550 N. Torrey Pines Road, La Jolla, CA, 92037, USA

#Yumi Won and Hyunwoo Jeon contributed equally

*Corresponding author: Hyungdon Yun, Department of Systems Biotechnology, Konkuk University, 120 Neungdong-ro, Gwangjin-gu, Seoul, 05029, Korea.

E-mail: hyungdon@konkuk.ac.kr

Materials

The *E. coli* JW2581 Tyr auxotroph was obtained from *E. coli* Genetic Stock Centre, Yale University, New Haven, USA. The plasmids pHCE-IIB and pD422-NH were purchased from Bio-Leaders (Seoul, Korea) and ATUM (California, USA) respectively. Pyrocatechol, 2-fluorophenol, 3-fluorophenol, 2, 3-fluorophenol, 2, 6-fluorophenol, 2,3,6-fluorophenol, 2,3,5,6-fluorophenol, L-Dopa, 3-fluorotyrosine were purchased from Sigma-Aldrich. Ni-NTA affinity columns were purchased from Qiagen (Valencia, CA, USA). All the other chemicals like pyruvate, acetophenone, pyridoxal 5'-phosphate and amino donors were purchased from Sigma-Aldrich, Korea.

Construction of plasmids and strains

DNA manipulations were performed according to the procedures described by TaKaRa (Kusatsu, Japan). PCR reaction (50 μ l) contained 0.1 μ M of each primer, 50 ng of template DNA, 1X LA PCR buffer II (Mg²⁺ plus), 0.2 U of TaKaRa LA Taq and 0.2 mM of each deoxyribonucleotide triphosphates. DNA amplification was performed in a DNA thermal cycler (Master gradient thermal cycler, Eppendorf, Hamburg, Germany) programmed for an initial denaturation (94°C for 1 min), followed by 30 cycles of chain reaction for 1 min at 94°C, 1 min at 58°C and 2 min at 72°C with an extension at 72°C for 10 min. For construction of a plasmid pHCEIIB harboring TPL, TPL was amplified as mentioned above and subsequently cloned into pHCEIIB using *Kpn*I and *Bam*HI restriction enzymes. In order to clone the target proteins (GFP and TAST) into pD422-NH, target proteins were amplified as mentioned above and subsequently cloned into pD422-NH using *Sap*I restriction enzyme. These plasmids harboring the target proteins were co-transformed into *E. coli* JW2581 tyrosine auxotroph. All the constructs were sequenced and confirmed for their target protein sequences.

Table S1. Selection of suitable cell system for the biosynthesis Tyr analog and its residue specific incorporation into target protein.

	Sr. No	Construct	Description				Comments
			Promoter	Inducer	Replication Origin	Antibiotic resistance	
Double Induction System	1.	pBAD33-TPL	araBAD	Arabinose	PBR322	Cm	Off-white coloured cells
		pQE80L-GFP	T5	IPTG	Col E1	Amp	
	2.	pQE80L-TPL	T5	IPTG	Col E1	Amp	Off-white coloured cells
		pBAD33-GFP	araBAD	Arabinose	PBR322	Cm	
Single Induction System	3.	pHCEIIB-TPL	HCE	-	pUC	Amp	Orange-red coloured cells with partially incorporated Tyr.
		pD422-NH-GFP	T5	IPTG	p15A	Zeo	

Double induction system

Gene encoding TPL was cloned into pBAD33 (pBAD33-TPL) and that for GFP into pQE80L (pQE80L-GFP). Both the vectors were co-transformed into *E. coli* Tyr auxotroph. We anticipated to achieve the expression of TPL in the first phase, followed by Dopa biosynthesis and its incorporation into GFP (termed as GFP-bDopa) in second phase. However, the anticipated orange-red color of the harvested cells was not observed. Also, SDS-PAGE demonstrated the successful expression of only TPL but not GFP (Figure S1). The expression of TPL and Dopa biosynthesis was confirmed by TPL activity test,¹ which confirmed the biosynthesis of 2.1 mM Dopa (Figure S2). These results indicated that although Dopa was biosynthesized, it did not incorporate into GFP in the absence of tyrosine. Hence, to construct a new cell system, we switched the vectors with respect to protein expression (pQE80L-TPL and pBAD33-GFP) in *E. coli* Tyr auxotroph. However, the newly developed cell system also enabled the expression of only TPL but not GFP (Figure S1).

Single Induction system

We further aimed to develop a 'one inducible vector system' using constitutive promoter to express TPL and T5 promoter to express GFP. For TPL expression, a new vector pHCEIIB with a constitutive promoter was selected. pD422-NH with T5-inducible promoter was used for GFP expression (Table S1). Both the vectors were co-transformed into *E. coli* Tyr auxotroph. Cells were cultivated till OD₆₀₀=1.0 to achieve TPL expression in M9 minimal media with limited Tyr (0.1 mM). The cells were washed and shifted to the Tyr deprived-M9 minimal media supplemented with pyrocatechol and pyruvate to achieve Dopa biosynthesis for 30 min, and its direct incorporation into

GFP was performed by adding IPTG. After 12 h incubation using this cell system, orange-red color of the harvested cells was obtained, indicating the incorporation of biosynthesized Dopa into GFP. The expression of TPL and GFP was also confirmed by SDS-PAGE (Figure S1). These results encouraged us to further optimize the experimental protocol using fluorescence intensity analysis. It was estimated that higher the biosynthesis of Dopa, higher would be the incorporation efficiency and thus fluorescence intensity.

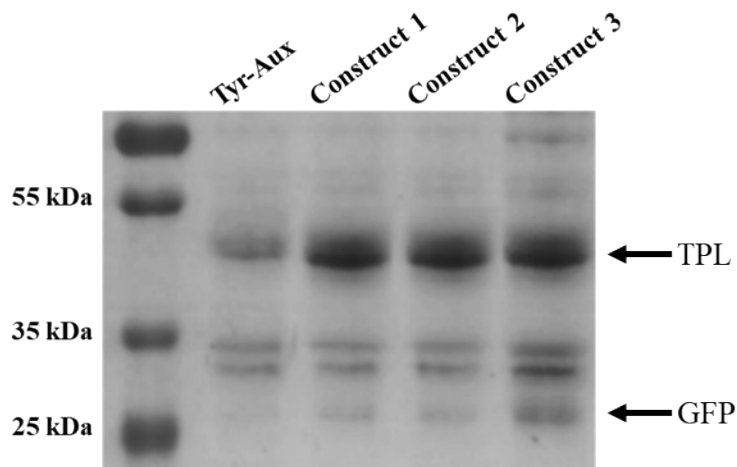


Figure S1. Coomassie-stained SDS-PAGE showing expression of TPL in all three constructs but absence of GFP expression in constructs 1 and 2 due to failure in biosynthesized Dopa incorporation. Third construct demonstrates TPL as well as GFP expression indicating Dopa biosynthesis and its residue specific incorporation into GFP in absence of Tyr.

Construct 1: *E. coli*. Tyr auxotroph harboring pBAD33-TPL and pQE80L-GFP.

Construct 2: *E. coli*. Tyr auxotroph harboring pQE80L-TPL and pBAD33-GFP

Construct 3: *E. coli*. Tyr auxotroph pHCEIIB-TPL and pD422-NH-GFP

Estimation of L-Dopa biosynthesis using TPL

TPL activity test is nothing but the measure of Dopa biosynthesis as a function of time. The TPL activity was determined by performing 5 mL whole cell reaction containing 100 mM Tris-HCl buffer (pH 8.0), 20 mM Pyrocatechol, 30 mM pyruvate, 22 mM Ammonium chloride (NH_4Cl), 8 mM Ammonium sulphate ($(\text{NH}_4)_2\text{SO}_4$) and 10 mM Ascorbic acid at 30 °C. Enzyme reaction was stopped by adding 10% perchloric acid and centrifuged (13,000 rpm, 30 min). Samples were then analyzed using HPLC. The quantitative analysis of biosynthesized L-Dopa was performed using YL9100 HPLC system with YL9110 quaternary pump and YL9120 UV-visible detector connected with C_{18} Symmetry column (Waters, MA). Elution was performed with solvent A - 0.1% Trifluoroacetic acid in water (TFA) and solvent B- methanol with an isocratic elution 99:1 (A: B) for 30 min at 280 nm wavelength and 1 mL/min flow rate. At 3 h of reaction 1.5 mM of Dopa was quantified by HPLC. The highest concentration of Dopa biosynthesized at 6 hours was quantified as 2.1 mM which was 33 % higher compared to that of 3 hours. But it should be also noticed that, after 6 h to 15 h Dopa concentration was decreased by 33 % to 1.4 mM (Figure S2). As Dopa biosynthesis is a reversible reaction so TPL can further cleave the biosynthesized Dopa into its substrates.

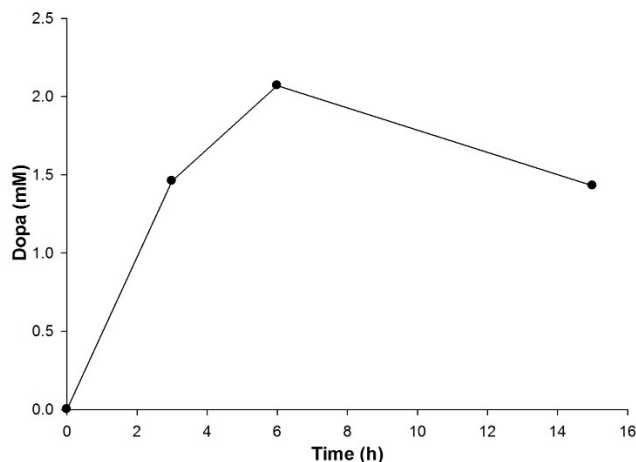


Figure S2. Estimation of Dopa biosynthesis (5 mL whole cell reaction containing 100 mM Tris-HCl buffer pH 8.0, 20 mM Pyrocatechol, 30 mM pyruvate, 22 mM NH₄Cl, 8mM (NH₄)₂SO₄ and 10 mM Ascorbic acid at 30 °C)

Amino acid sequence of TPL from *Citrobacter freundii*¹

MNYP AEPFRIKSVETVSMIPRDERLKKMQEAGYNTFLNSKDIYIDLTTDSGNTAMSDKQWAGMMMGDEAYAGSENFYHLERTVQELFGFKHIVPTHQGR
 GAENLLSQLAIKPGQYVAGNMYFTTRYHQEKNGAVFVDIVRDEAHDAGLNIAFKGDIDLKLLQKLIDEKGAENIAYICLAVTVNLAGGQPVSMANMRAVR
 ELTEAHGKIVFYDATRCVENAYFIKEQEQGFENKSIAEIVHEMFYADGCTMSGKKDCLVNI GGFLCMNDDEM FSSAKELVVVYEGMPSPSYGGLAGRDMEA
 MAIGLREAMQY EYIEHRVKQVRYLGDKLAAGVPIVEPVGGHAVFLDARRFCEHLTQDEFPAQSLAASIYVETGVRSMERGIISAGRNNVTGEHHRPKLETV
 RLTIPRRVYTYAHMDVVADGIIKLYQHKEDIRGLKFIYEPKQLRFFFTARFDYI

Amino acid sequence of GFP²

MSKGEELFTGVVPIVELDGDVNGHKFSVRGEGEGDATNGKITLKICTTGKLPVPWPVLVTTTCGYGVQCFARYPDHMKRHHDFKSA MPEGVQERTISFKD
 DGTFKTRA EVKFEGDTIVNRIKLGIDFKEDGNILGHKLEYNFNSHKVYITADKQKNGIKANFKIRHNVEDGVSQ LADHYQQNTPIGDGPVRLPDNHYLSTQS
 VILEDPNEKRDHMLHEFVTAAGITHGMDELYK

(Number of Tyrosine (Y) residue: 8)

Amino acid sequence of ω-TA from *Sphaerobacter thermophilus* (ω-TAST-I).³

MSSGSRGGNVYREPGSVAADL FERARRVLP GGNTTRTTVYSAPYPPYAARGGAVIVDADGEERLDFVNNY TALIHGHADPDINEAVIRQLADGVAFAMP
 TEHEIALAELLTERVPSLQQVRFTNSGTEAVMMAIKAARAYTGRPRIAKFDGCYHGSYDFAEVSTQSSGKPGEDGFPVATPYTGGTPQAVLDSVVVLPFNDI
 DGTERLIEQHRDELA AVLIDPNRSLGLYPAEPAFLQRLREITRAYGIVLIFDEVISLRSYGGMQSVLGVTPDLTAMGKIIGGGFPVGAVGGS AEVMSVFDPT
 GGPPRAPHGGTFNANPVTMVAGLTAMRKLTPAEFDRLATLGQQLRAGVEEVLREAGVPGQVTGYGSLFHIHLHQRPLADYRNSVLSAQERAFVGRVHEAL
 MGRGIFITPALFGCLSTPMGVPEVEAFVDAFAAALQDARG

(Number of Tyrosine (Y) residue: 14)

Amino acid sequence of ω-TA from *Sphaerobacter thermophilus* (ω-TAST-II)

MNQTGAAQETWNTADLVRKDKAHMLHPVSNLRQLQEY GALVMARGEGVYLWDTDGKRYIDAFAGLWNVNVVGHGRRELADAMREQGERLAFSPTFFG
 LATPPTIELAAKLASLFPGLDLYNFNTSGGAESNETAIKIARYY WALRGKPKVKVLSRMMAYHGIAMGALSATGIPAYWQDFGPRPAGFIHLTPPYRHHG
 EGMTEDEFVDSLVRLEETIQREGADTIAAFIGEP IQGAGGVVPPDRYWP AIAEVLRRHDILLI LDEVITGFGRTGTLFGMQQYGITP DIVSFAKGVTSGYVPL
 GGVGVSSKIFDVLAEPDRVFMHGFTYSGHPVACAVARNIQIEEENLAANAGEVGAYMIGELSKLLERPYVGNVRGKGLMMLVELVADKETKAKFDPAQN
 LGGRLQAATRKRGIIVRCNPDSIAIAPPLILTKEEASTVVEAIAADSLTEVLG

(Number of Tyrosine (Y) residue: 17)

Amino acid sequence of alanine dehydrogenase from *Bacillus subtilis* (AlaDH)

MIIGVPKEIKNNENRVALTGGVSQLISNGHRVLVETGAGLGSGFENEAYESAGAEIADPKQVWDAEMVMKVKEPLPEEYVYFRKGLVLFYTLHLAAEPELA
QALKDKGVTAIAYETVSEGRTPLLTPMSEVAGRMAAQIGAQFLEKPKGGKILLAGVPGVSRGKVTIIGGGVGTNAAKMAVGLGADVTIIDLNADRLRQL
DDIFGHQIKTLISNPVNIADAVAADLLICAVLIPGAKAPTLVTEEMVKQMKPGSVIVDAIDQGGIVETVDHITTHDQPTYEKHGVVHYAVANMPGAVPRT
STIALTNVTPYALQIANKGAVKALADNTALRAGLNTANGHVTYEAVARDLGYEYVPAEKALQDESSVAGA

(Number of Tyrosine (Y) residue: 11)

General protocol for the biosynthesis Tyr analogs and their incorporation into enzyme/protein

A single colony of host cell harboring plasmids pHCEIIB-TPL and pD422NH-GFP/ ω -TAST-I/ ω -TAST-II/AlaDH was inoculated into 10 mL M9 minimal media (M-I) supplemented with 0.4% (w/v) of glucose, 0.1 mM of CaCl₂, 1.0 mM of MgSO₄, 25 μ g/mL of thiamine, 19 amino acids (40 mg/L) and 0.1 mM Tyr. 1-1.5% starter culture was added to 500 mL of fresh M-I, pH 7.4 with 0.1 mM Tyr, in Erlenmeyer flask along with respective antibiotics and incubated at 37 °C with shaking at 200 rpm to attain cell OD₆₀₀ = 1.0. These cells were centrifuged at 5000 rpm, 4 °C for 10 min and washed with 0.9% NaCl and transferred to another 500 mL M-I, pH 8.0 without adding Tyr. To biosynthesize Tyr analogs, optimized concentration of substrates for respective Tyr analogs were supplemented to the media and incubated at 30 °C with shaking at 200 rpm for 30 min. Further protein expression was induced by adding 0.5 mM IPTG and incubated at 30 °C for next 12 hours with shaking at 120 rpm. Harvested cells were stored at -20°C till further use.

Fluorescence analysis

Fluorescence analysis was performed for the whole cells (OD₆₀₀=1) and the purified enzyme samples diluted in 10 mM HEPES buffer pH 7.4. Fluorescence measurements were recorded on a fluorescence spectrometer (SHIMADZU- RF-5310PC) by exciting the samples at 485 nm and measuring the fluorescence emission in a range 500 - 600 nm.

Metal biosensing using fluorescence spectroscopy²

Metal ion screening was performed for the protein samples (GFP, GFP-Dopa and GFP-bDopa) diluted in 10 mM HEPES buffer pH 7.4, against 0.1 mM of different metal ions such as Na⁺, Mn²⁺, Mg²⁺, K⁺, Cu²⁺ and Ca²⁺. Copper titration experiments were carried out to determine the concentration dependent fluorescence quenching of protein samples. To perform the concentration dependent fluorescence quenching study, 100 μ L of 3 μ M GFP-bDopa were treated with 100 μ L of different concentrations of copper solutions, respectively. The reversibility of the sensors was assessed by the addition of 1 mM of metal chelator, ethylenediamine tetra acetic acid (EDTA) to the copper treated GFP, GFP-Dopa and GFP-bDopa solutions.

Enzyme assay ω -transaminase

The activity of ω -TAST towards various substrates was determined by performing an enzyme reaction in 500 μ L volume containing 100 mM Tris-HCl buffer (pH 8.0), 10 mM amino donor, 10 mM pyruvate, 0.1 mM PLP and ω -TAST 0.05 – 0.5 mg/ml at 37 °C for 30 min. Enzyme reaction was stopped by adding 10% perchloric acid and centrifuged (13,000 rpm, 30 min). The quantitative analysis of biosynthesized products was performed using YL9100 HPLC system with YL9110 quaternary pump and YL9120 UV-visible detector.

Analysis of pyruvate, acetophenone, rac-methylbenzylamine by HPLC

Substrate	Column	Buffer	Flow rate	Detection wavelength	Retention time
Acetophenone	C ₁₈ Symmetry column	45% MeOH (0.1% TFA) and 55% water (0.1% TFA)	1.0 mL/min	254 nm	10 min
Pyruvate	Amine X HPX-87H HPLC column	5 mM sulfuric acid	0.6 mL/min	210 nm	8 min
rac-MBA	Crownpak CR column	Perchloric acid (pH 1.5)	0.6 mL/min	210 nm	45 min

Enzyme assay of Alanine dehydrogenase

The activities of Alanine dehydrogenase (AlaDH) was determined using an NADH-dependent (340 nm, $\lambda_{340} = 6220 \text{ M}^{-1}\text{cm}^{-1}$) spectrophotometric assay. Activity is calculated from the stoichiometric oxidation of NADH as measured by the change in absorbance

over time. One unit of activity is defined as the amount of enzyme that catalyzes the formation of 1 μmol of NADH. AlaDH activity assay was carried out in 100 mM Tris-HCl buffer (pH 8.0) containing AlaDH (0.0005 - 0.01 mg/mL), 10 mM substrate, and 1 mM NAD⁺ at 37 °C.

Optimization of substrate concentration for the biosynthesis of L-Dopa and its incorporation

To achieve the maximum intracellular TPL-catalyzed biosynthesis of Dopa and its efficient incorporation into GFP, concentration of pyrocatechol and pyruvate was optimized. Experiment with varying concentrations of pyrocatechol resulted in considerable difference in the intracellular biosynthesis of Dopa and its incorporation. Dopa biosynthesis and its concurrent incorporation into GFP was achieved at varying concentrations of pyrocatechol (0, 5, 10, 20, and 30 mM). GFP-bDopa expression levels at different concentrations of pyrocatechol were determined by fluorescence spectrophotometer and SDS-PAGE. Fluorescence emission spectra of bacterial cells (OD₆₀₀ = 1) expressing target proteins were generated. The highest intensity of protein expression was observed in the cells exposed to 20 mM pyrocatechol concentration followed by 10-, 30- and 5-mM (Figure S3-A). The evident ~27 kDa Coomassie-stained bands in lanes 3, 4, 5, and 6 indicated the expression of GFP-bDopa (Figure S3-B). The highest expression of GFP-bDopa was observed at 20 mM concentration of pyrocatechol reflecting similar results to that of fluorescence emission (lane 5, Figure S3-B). Additionally, the bands at ~52 kDa in Lanes 2, 3, 4, 5 and 6 demonstrated the expression of TPL. In absence of pyrocatechol (lane 2) neither GFP-bDopa nor GFP expression was observed (Figure S3-B)

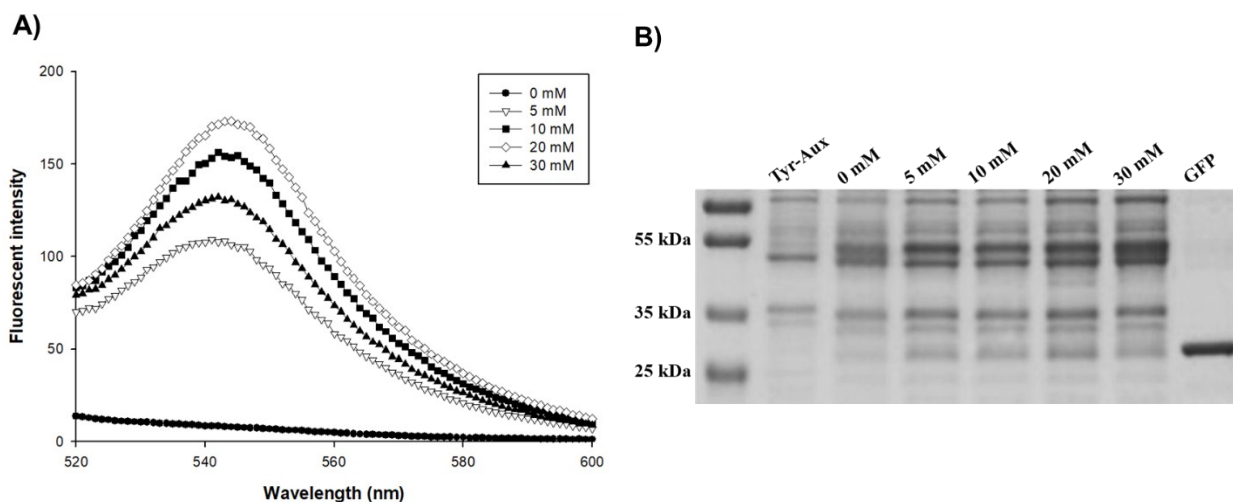


Figure S3. A) Effect of pyrocatechol concentration on Fluorescence emission spectra of whole-cells (OD₆₀₀=1) expressing GFP-bDopa (Excitation wavelength = 485 nm); B) Coomassie-stained SDS-PAGE showing optimum concentration of pyrocatechol for the intracellular biosynthesis of Dopa and its incorporation into GFP.

Next, we optimized pyruvate concentration for Dopa biosynthesis at different concentrations (0, 5, 10, 15 and 20 mM). Surprisingly, GFP-bDopa expression was not influenced by absence/presence of exogenously supplied pyruvate (Figure S4) as it is metabolically produced by *E. coli*

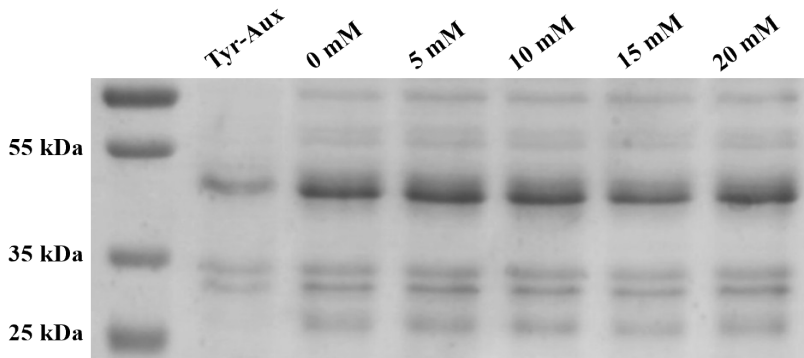


Figure S4. Coomassie-stained SDS-PAGE showing pyruvate concentration independent intracellular biosynthesis of Dopa and its incorporation into GFP

pH, time and temperature optimization

The effect of pH on the intracellular biosynthesis of DOPA was studied at different pH conditions (pH 7.0, 7.5, 8.0 and 8.5). The harvested cells from each pH condition with Dopa incorporated GFP ($OD_{600} = 1$) were analyzed for fluorescence emission. Higher the Dopa biosynthesis higher would be the incorporation efficiency and thus fluorescence intensity. Cells harvested at pH 8.0 showed highest fluorescence intensity followed by that at pH 7.0, 7.5 and 8.5 (**Figure S5-A**). Thus, we confirmed that pH 8.0 was optimum for TPL-catalyzed biosynthesis of Dopa. The optimum temperature for bacterial cell growth and TPL expression has been reported to be 37 °C. However, the biosynthesis of Dopa was more efficient at 30 °C. To confirm the effect of varying temperatures, the cells were cultured at 30 and 37 °C. Also, the effect of temperature on the IPTG-induced GFP expression with respect to time was monitored. Fluorescence emission spectra of the cells ($OD_{600} = 1$) exhibited temperature of 30 °C, following the incubation for 12 h after IPTG induction, was optimum for the biosynthesis of Dopa and its concurrent incorporation (**Figure S5-B**).

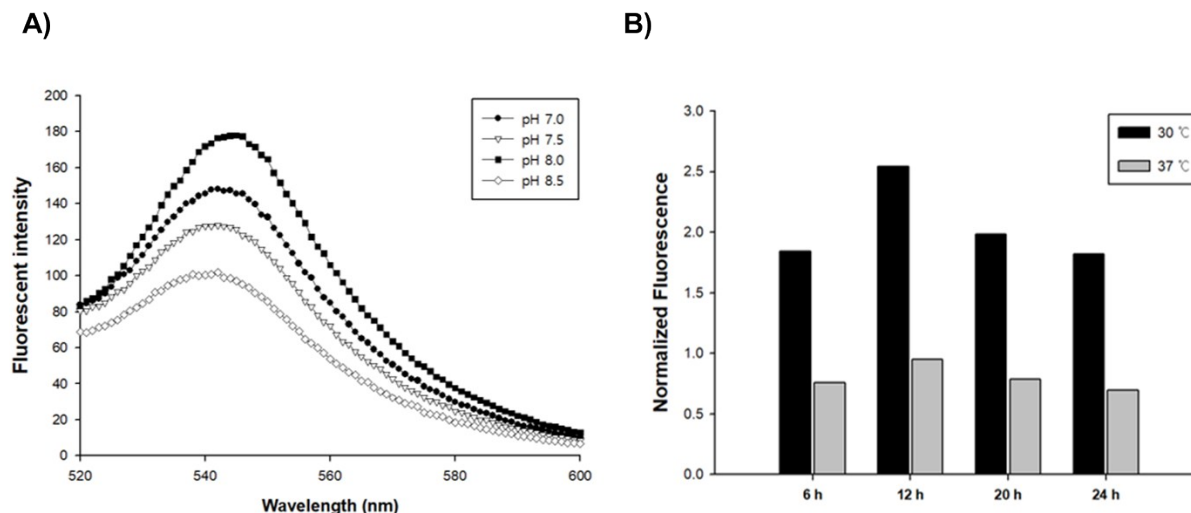


Figure S5. A) Fluorescence emission spectra of proteins expressed at different pH conditions. B) Expression level of GFP-bDopa at different time intervals and temperature conditions

Protein purification and Fluorescence studies

The target proteins were purified using the previously reported protocols.⁴ Briefly, after the overnight induction at 30°C, the cells expressing target proteins were harvested by centrifugation (5000 rpm, 10 min) and washed twice with 100 mM Tris/HCl buffer (pH 8.0). The washed cells were collected by centrifugation and resuspended in 10 mL lysis buffer [Na_2HPO_4 (50 mM), NaCl (300 mM), Imidazole (5 mM, pH 8.0)]. The cell suspension was then subjected to ultrasonic disruption by a horn-type sonicator (Sonic& Material Inc, USA). During sonication, the sample tube containing the cell mass suspension was held in an ice bath. The sonication was carried for the total duration of 30 min, with a duty cycle of 37.5%. The His6-tagged enzyme from the cell lysate was purified at 4°C on a Ni-NTA agarose resin [Qiagen, Hilden, Germany].⁴ The enzymes were eluted with the increasing gradient of imidazole [50-250 mM]. The eluted solution containing the purified protein was dialyzed against 20 mM Tris-HCl buffer (pH 8.0) and concentrated using an Amicon PM-10 ultrafiltration unit. Glycerol (25% v/v) was added to the purified enzyme solution and stored at -20 °C for further study.⁴ Homogeneity of the purified proteins were determined by SDS-PAGE (**Figure S6B**).

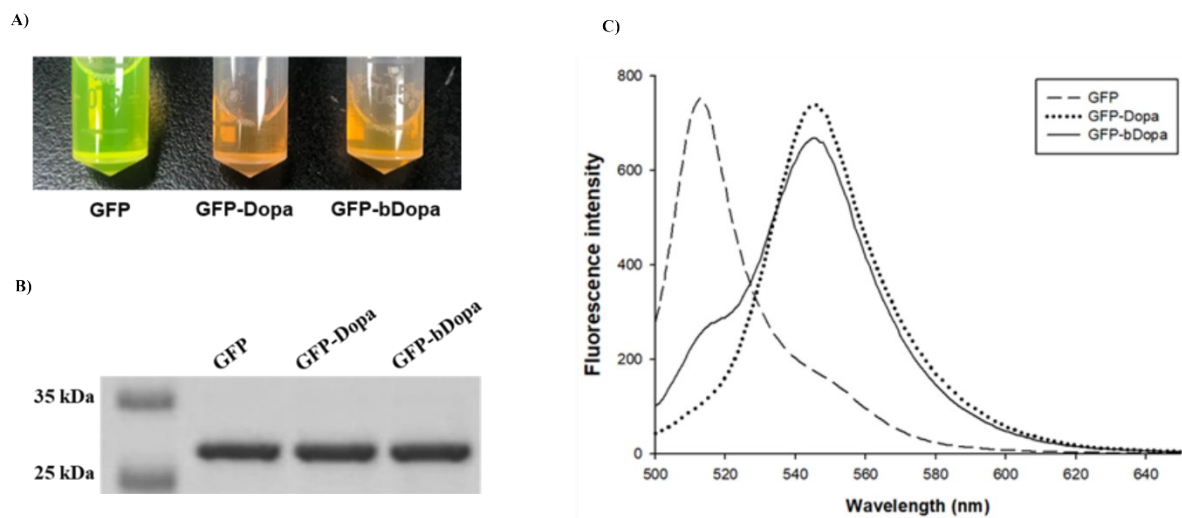


Figure S6. A) Visual color difference between GFP, GFP-Dopa and GFP-bDopa; B) Coomassie-stained SDS-PAGE showing purified proteins GFP, GFP-Dopa and GFP-bDopa C) Fluorescence emission spectra of GFP λ_{max} = 513nm, GFP-Dopa (λ_{max} =547nm) and GFP-bDopa (λ_{max} = 546nm);

Intact Protein Mass Spectrometry⁵

Purified proteins were diluted using mass spec grade water (0.1 mg/mL). 5 mL (ca. 500 ng) sample was analyzed on a Waters I-Class LC connected to a Waters G2-XS time of flight (TOF) mass spec. LC conditions: Waters BEH C18 column (2.1x55 mm, 1.7 mm, 300 Å), 0.4 mL/min, 0.4 minute isocratic hold followed by a 5-99% B gradient over 4.6 minutes (A: 0.1% FA in H₂O; B: 0.1% FA in ACN). MS conditions and data processing: ESI+ ionization (m/z 500-2000), spectral combine across the main peak area, deconvolution to neutral mass using Waters MaxEnt1.

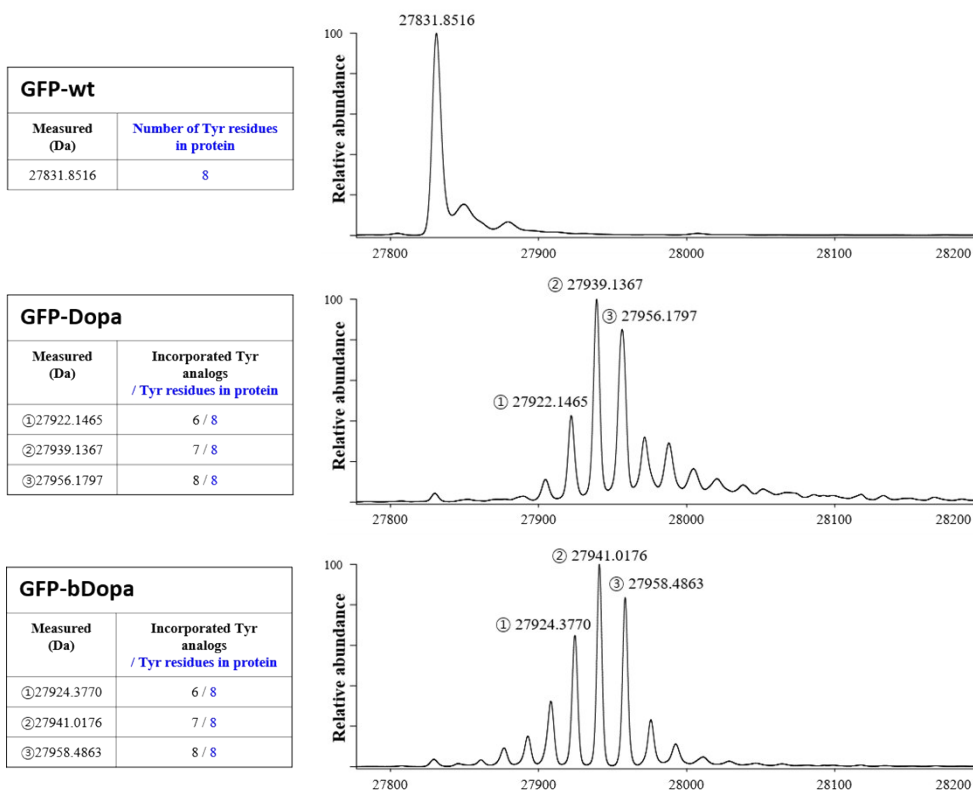


Figure S7. B) Quantitative High-Resolution Mass Spectrometry of Intact Proteins, GFP, GFP-Dopa and GFP-bDopa. The predicted molecular weights of are 27832.41 Da, 27960.33 Da and 27960.338 Da, respectively. The measured molecular weights are shown in the figure

Metal bio-sensing using fluorescence spectroscopy

Our previous work surmised that coordination of Cu^{2+} and Dopa contribute to the fluorescence quenching of GFP-Dopa.² In order to confirm the efficiency of GFP-bDopa functionality similar to that of GFP-dopa as a Cu^{2+} biosensing tool we performed following sets of experiments. Initially, we evaluated the effect of various metal ions (0.1 mM) on GFP, GFP-Dopa and GFP-bDopa (Figure S8A). The results suggested that fluorescence intensity decreased with the increasing concentration of Cu^{2+} . While the fluorescence intensity exhibited by GFP-bDopa was ~ 280 in the absence of Cu^{2+} , it steeply decreased to ~ 50 in the presence of $50 \mu\text{M}$ Cu^{2+} (Figure S8B). Furthermore, it was found that the addition of metal chelator such as EDTA reverses the quenching of fluorescence consequent of the binding of Cu^{2+} ions to biosynthesized GFP-bDopa and thereby confirming that fluorescence quenching was resultant due to the binding of Cu^{2+} ions (Figure S8C).

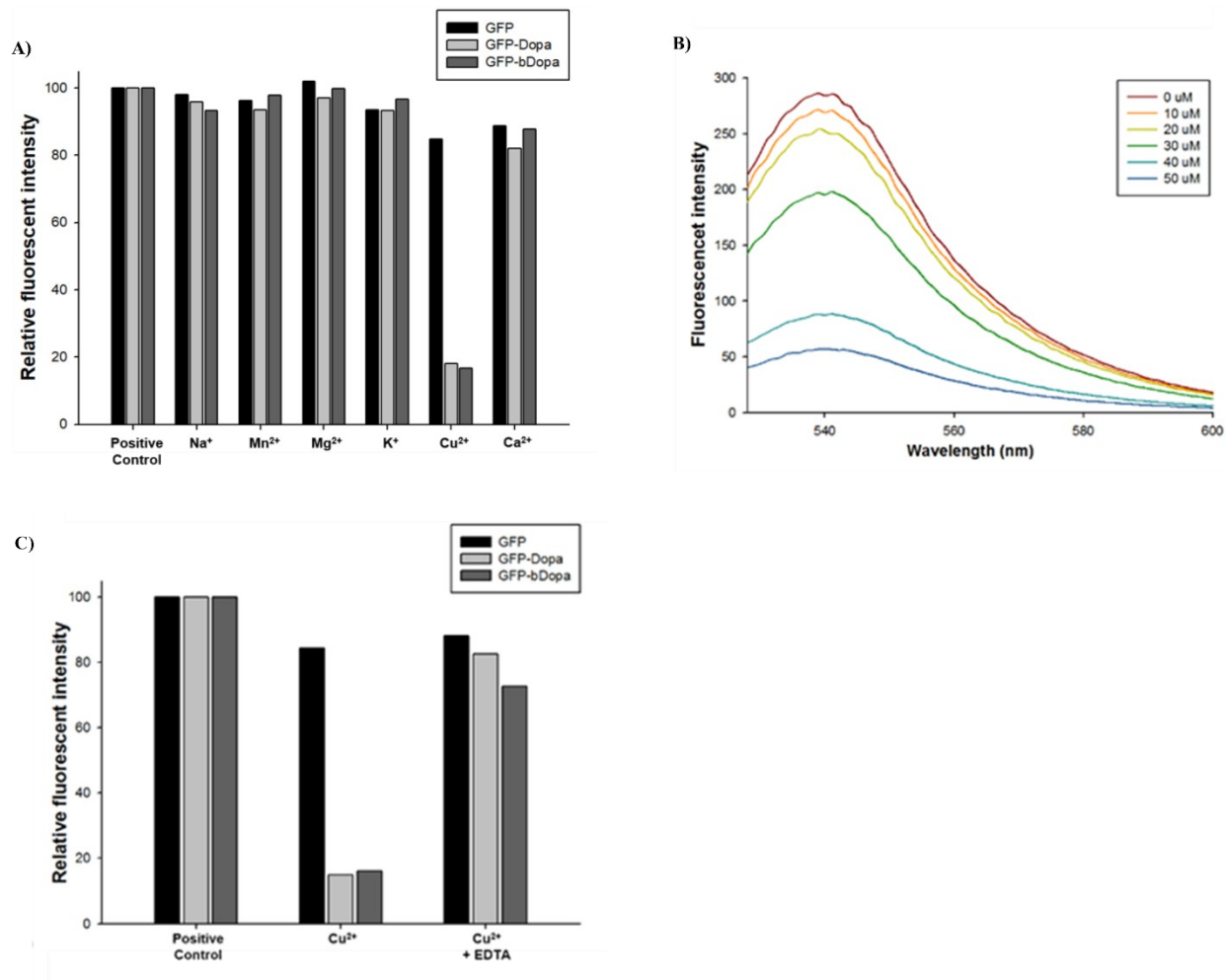


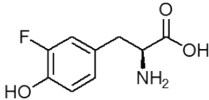
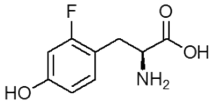
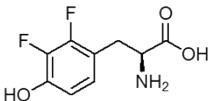
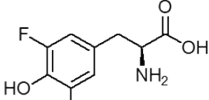
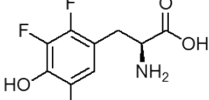
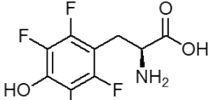
Figure S8. A) Effect of different metal ions on the fluorescence emission of GFP, GFP-Dopa and GFP-bDopa. B) Concentration dependent fluorescence quenching of GFP-bDopa in presence of Cu^{2+} ; C) The reversibility assessment by the addition of 1 mM of metal chelator (EDTA) to the copper treated protein samples.

Optimization of substrate concentration for the biosynthesis of FYs and their incorporation into GFP

Preliminary experiments suggested that 20 mM pyrocatechol was optimum for the biosynthesis of Dopa. But, 20 mM fluorophenol concentration was found to be highly toxic to the cells in case of FYs. Hence, the optimum concentration of fluorophenols for the biosynthesis of FYs and their incorporation target protein was determined as discussed for that of Dopa. The results of these experiments suggested that 3 mM concentration of all the fluorophenols was optimum for the biosynthesis of corresponding FYs and their incorporation into a target protein (Figure S9). The increase in the concentration of fluorophenols resulted in the decrease in the

biosynthesis of corresponding FYs and their incorporation into GFP. pH, time and temperature conditions were determined as discussed that for Dopa. The whole cells expressing GFP mutants (GFP incorporated with various FYs) were analyzed for wavelength shift in emission spectra as a function of fluorine substitution (**Figure S10**). The pattern of wavelength shift was compared with the reported λ_{max} values (**Table S3**.)

Table S2. Phenol substrates used for the *in vivo* biosynthesis of corresponding fluorotyrosines and their incorporation into target proteins

Sr.No.	Phenol Substrate	Corresponding Tyrosine analogs
1	 2-fluorophenol	 3-fluorotyrosine (3-FY)
2	 3-fluorophenol	 2-fluorotyrosine (2-FY)
3	 2,3-difluorophenol	 2,3-difluorotyrosine (2,3-FY)
4	 2,6-difluorophenol	 3,5-difluorotyrosine (3,5-FY)
5	 2,3,6-trifluorophenol	 2,3,5-trifluorotyrosine (2,3,5-FY)
6	 2,3,5,6-tetrafluorophenol	 2,3,5,6-tetrafluorotyrosine (2,3,5,6-FY)

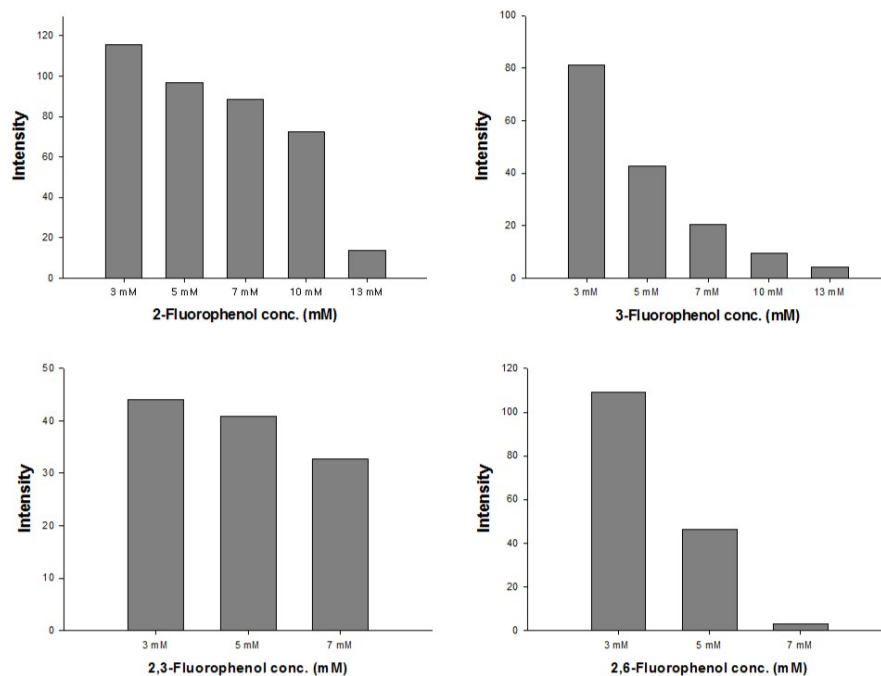


Figure S9. Relative fluorescence intensities of the of the FY's incorporated GFP expressed *E. coli* cells (OD₆₀₀ = 1)

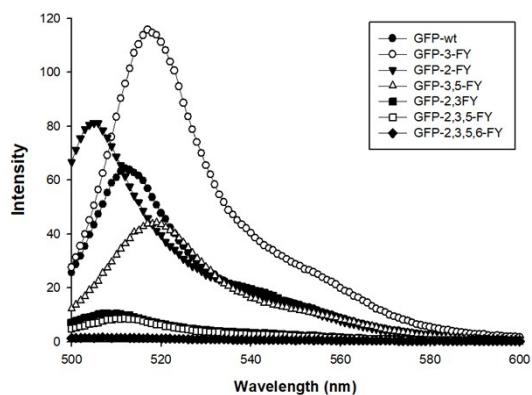


Figure S10. Fluorescence spectra of whole cells (OD₆₀₀ = 1) expressing GFP mutants and its comparison with wild type GFP.

Table S3. Wavelength shift pattern of the GFP based on flurotyrosine incorporation.

Mutant protein	Observed λ_{max} (nm)	Reported λ_{max} (nm)	Reference
GFP	512	507 nm/512 nm	6, 7
GFP-2-FY	505	-	-
GFP-3-FY	518	520	7
GFP-2,3-FY	508	506	6
GFP-3,5-FY	519	511	6
GFP-2,3,5-FY	512	512	6
GFP-2,3,5,6-FY	-	-	-

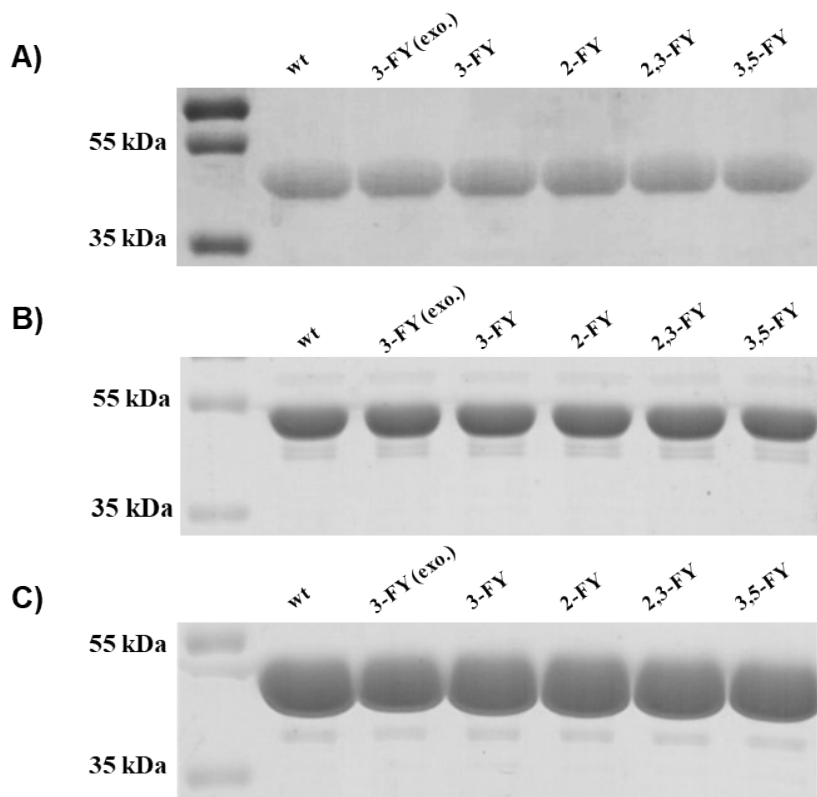


Figure S11. Coomassie-stained SDS-PAGE showing purified proteins A) ω -TAST-I (47 kDa); B) ω -TAST-II (47 kDa); C) AlaDH (40 kDa).

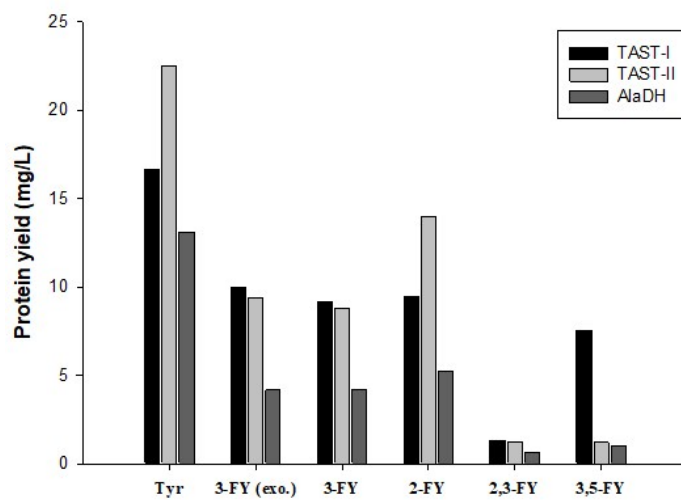
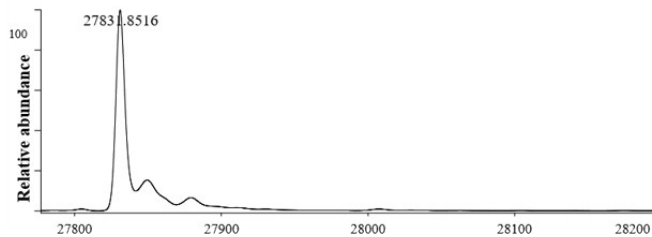


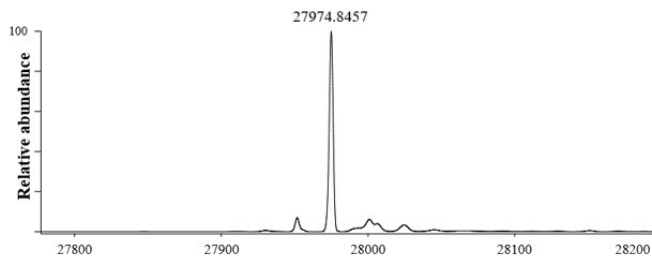
Figure S12. Protein yields of UAAs incorporated enzymes

A)

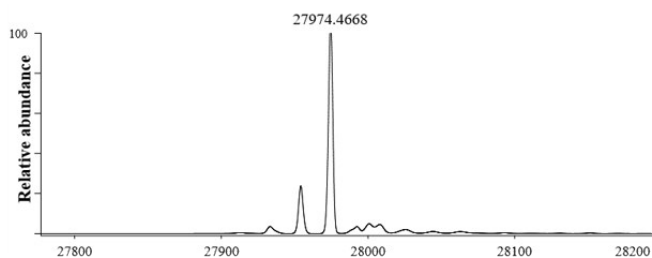
GFP-wt	
Measured (Da)	Number of Tyr residues in protein
27831.8516	8



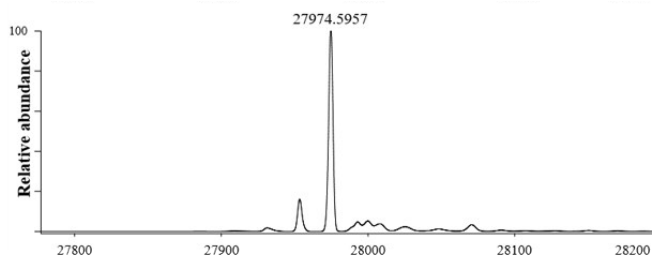
GFP-3-FY (exo.)	
Measured (Da)	Incorporated Tyr analogs / Tyr residues in protein
27974.8457	8 / 8



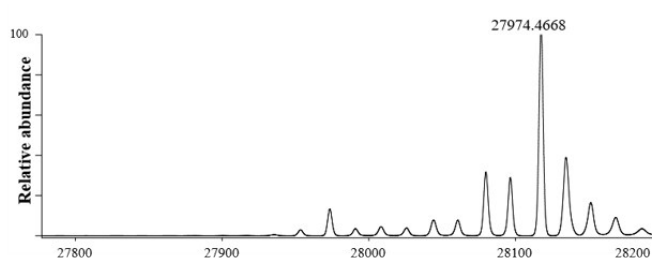
GFP-3-FY	
Measured (Da)	Incorporated Tyr analogs / Tyr residues in protein
27974.4668	8 / 8



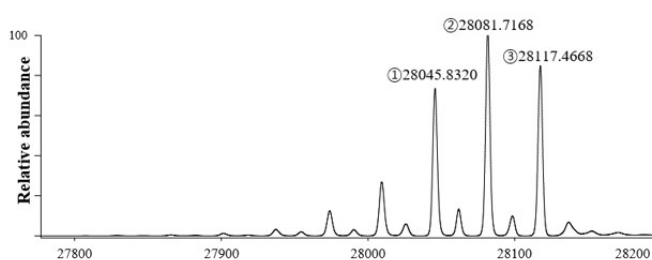
GFP-2-FY	
Measured (Da)	Incorporated Tyr analogs / Tyr residues in protein
27974.5957	8 / 8



GFP-2,3-FY	
Measured (Da)	Incorporated Tyr analogs / Tyr residues in protein
27974.4668	8 / 8

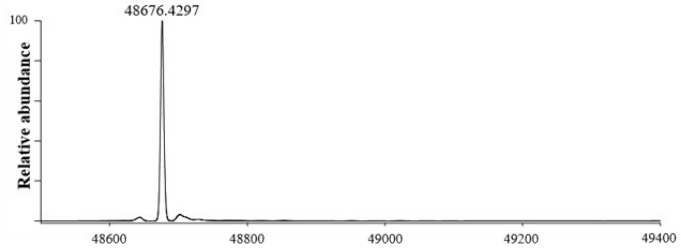


GFP-3,5-FY	
Measured (Da)	Incorporated Tyr analogs / Tyr residues in protein
①28045.8320	6 / 8
②28081.7168	7 / 8
③28117.4668	8 / 8

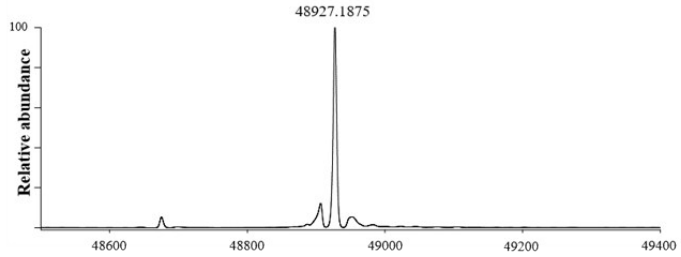


B)

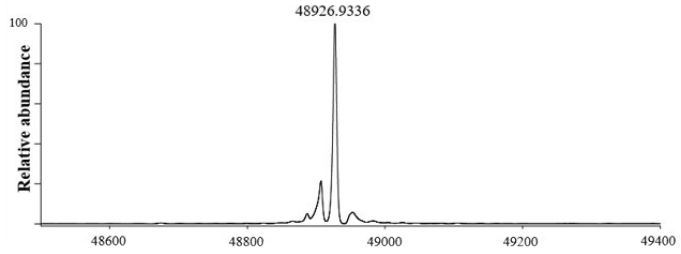
TAST-I-wt	
Measured (Da)	Number of Tyr residues in protein
48676.4297	14



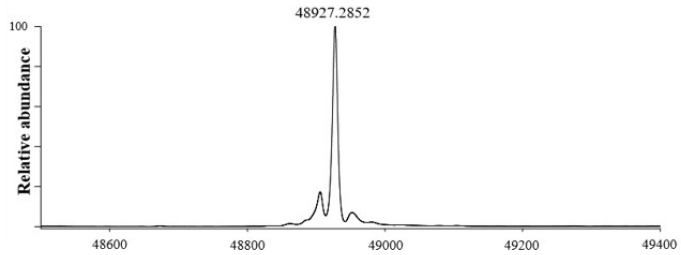
TAST-I-3-FY (exo.)	
Measured (Da)	Incorporated Tyr analogs / Tyr residues in protein
48927.1875	14 / 14



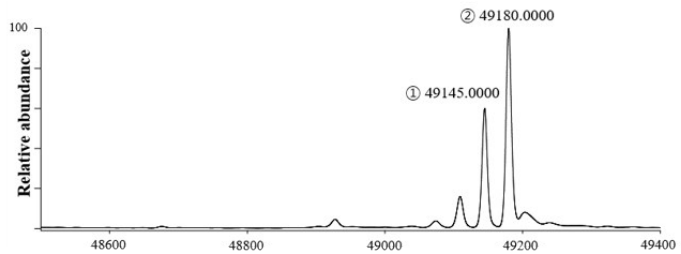
TAST-I-3-FY	
Measured (Da)	Incorporated Tyr analogs / Tyr residues in protein
48926.9336	14 / 14



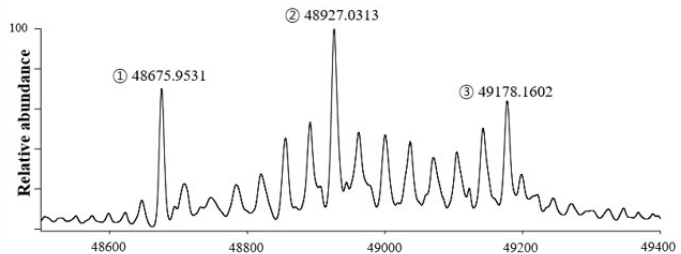
TAST-I-2-FY	
Measured (Da)	Incorporated Tyr analogs / Tyr residues in protein
48927.5852	14 / 14



TAST-I-2,3-FY	
Measured (Da)	Incorporated Tyr analogs / Tyr residues in protein
① 49145.0000	13 / 14
② 49180.0000	14 / 14

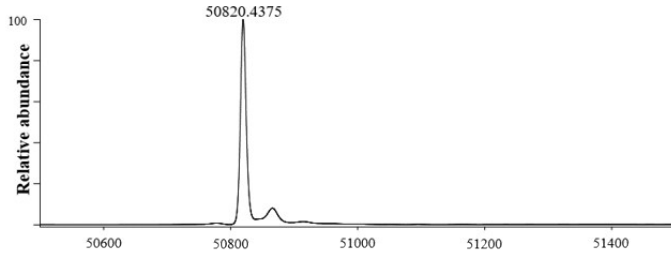


TAST-I-3,5-FY	
Measured (Da)	Incorporated Tyr analogs / Tyr residues in protein
① 48675.9531	0 / 14
② 48927.0313	7 / 14
③ 49178.1602	14 / 14

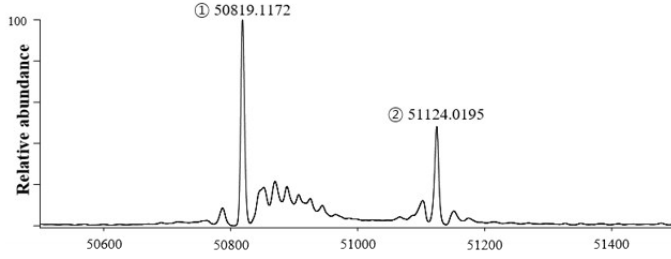


C)

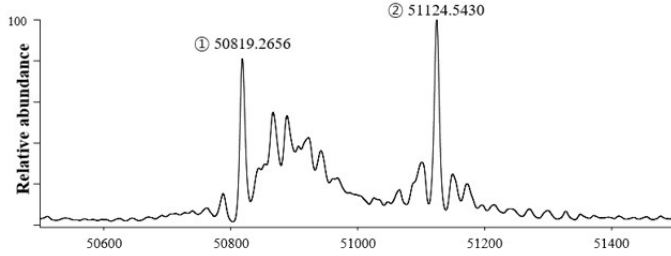
TAST-II-wt	
Measured (Da)	Number of Tyr residues in protein
50820.4375	17



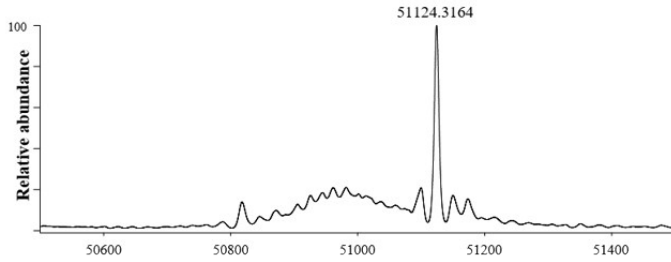
TAST-II-3-FY (exo.)	
Measured (Da)	Incorporated Tyr analogs / Tyr residues in protein
① 50819.1172	0 / 17
② 51124.0195	17 / 17



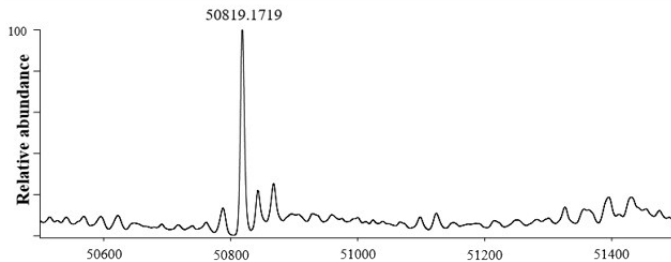
TAST-II-3-FY	
Measured (Da)	Incorporated Tyr analogs / Tyr residues in protein
① 50819.2656	0 / 17
② 51124.5430	17 / 17



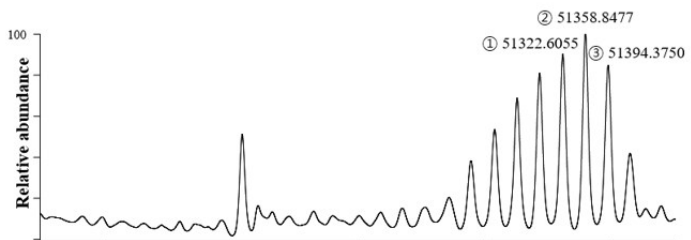
TAST-II-2-FY	
Measured (Da)	Incorporated Tyr analogs / Tyr residues in protein
51124.3164	17 / 17



TAST-II-2,3-FY	
Measured (Da)	Incorporated Tyr analogs / Tyr residues in protein
50819.1719	0 / 17

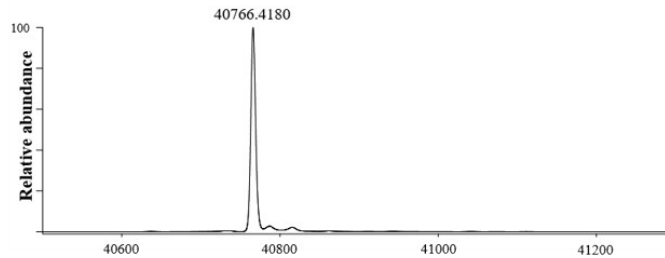


TAST-II-3,5-FY	
Measured (Da)	Incorporated Tyr analogs / Tyr residues in protein
① 51322.6055	15 / 17
② 51358.8477	16 / 17
③ 51394.3750	17 / 17

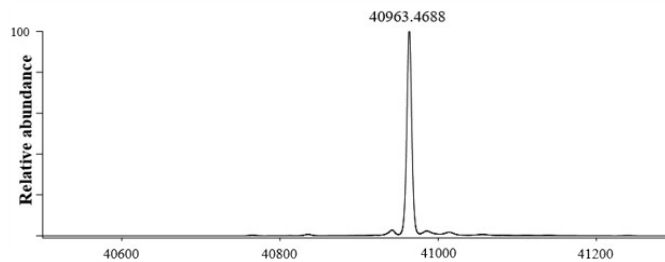


D)

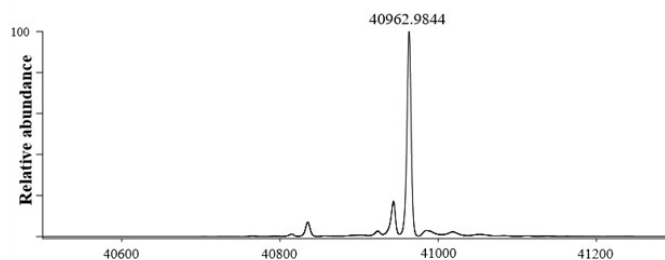
AlaDH-wt	
Measured (Da)	Number of Tyr residues in protein
40766.4180	11



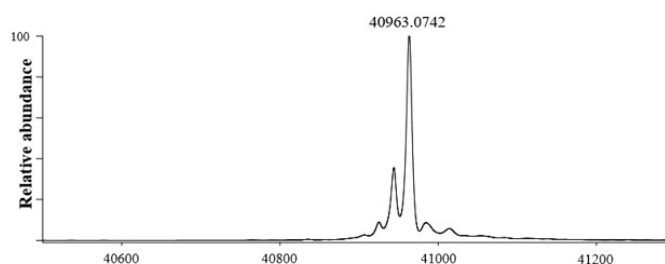
AlaDH-3-FY (exo.)	
Measured (Da)	Incorporated Tyr analogs / Tyr residues in protein
40963.4688	11 / 11



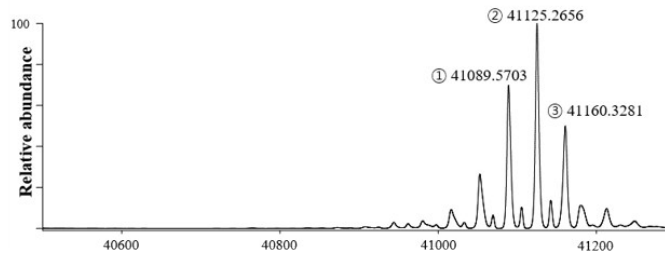
AlaDH-3-FY	
Measured (Da)	Incorporated Tyr analogs / Tyr residues in protein
40962.9844	11 / 11



AlaDH-2-FY	
Measured (Da)	Incorporated Tyr analogs / Tyr residues in protein
40963.0742	11 / 11



AlaDH-2,3-FY	
Measured (Da)	Incorporated Tyr analogs / Tyr residues in protein
① 41089.5703	9 / 11
② 41125.2656	10 / 11
③ 41160.3281	11 / 11



AlaDH-3,5-FY	
Measured (Da)	Incorporated Tyr analogs / Tyr residues in protein
41124.3477	10 / 11

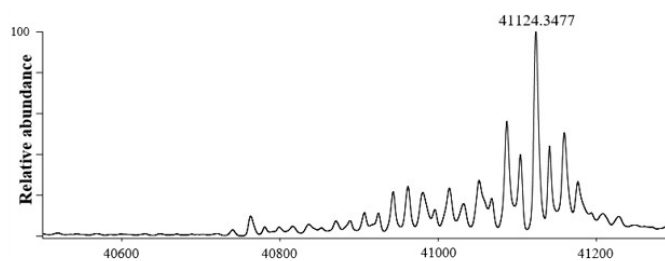


Figure S13. Quantitative High-Resolution Mass Spectrometry of Intact Proteins. **A)** Fluorotyrosine derivatives incorporated into GFP. **B)** Fluorotyrosine derivatives incorporated into TAST-I. **C)** Fluorotyrosine derivatives incorporated into TAST-II. **D)** Fluorotyrosine derivatives incorporated into AlaDH

Table S4. The calculated mass and measured mass of all the proteins used in the experiment are summarized. All purified proteins contained His tag. Δm denotes the difference between measured and calculated mass

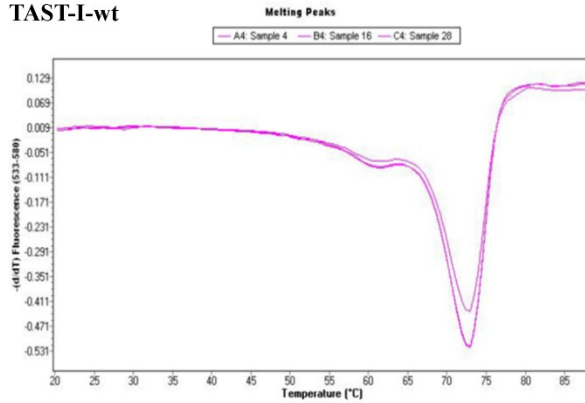
Name	Mass		Δm (Da)	Number of Tyr residues in protein	Number of incorporated Tyr analogs
	ⓐ Calculated (Da)	ⓑ Measured (Da)			
GFP-wt	27832.418	27831.8516	0.5664	8	-
GFP-Dopa	27960.338	27939.1367	21.2013		7
GFP-bDopa	27960.338	27941.0176	19.3204		7
GFP-3-FY (exo.)	27976.338	27974.8457	1.4923		8
GFP-3-FY	27976.338	27974.4668	1.8712		8
GFP-2-FY	27976.338	27974.5957	1.7423		8
GFP-2,3-FY	28120.258	28117.4238	2.8342		8
GFP-3,5-FY	28120.258	28081.7168	38.5412		7
TAST-I-wt	48675.9727	48676.4297	-0.457	14	-
TAST-I-3-FY (exo.)	48927.8327	48927.1875	0.6452		14
TAST-I-3-FY	48927.8327	48926.9336	0.8991		14
TAST-I-2-FY	48927.8327	48927.2852	0.5475		14
TAST-I-2,3-FY	49179.6927	49180	-0.3073		14
TAST-I-3,5-FY	49179.6927	48927.0313	252.6614		0
TAST-II-wt	50819.9688	50820.4375	-0.4687	17	-
TAST-II-3-FY (exo.)	51125.7988	50819.1172	306.6816		0
TAST-II-3-FY	51125.7988	51124.543	1.2558		17
TAST-II-2-FY	51125.7988	51124.3164	1.4824		17
TAST-II-2,3-FY	51431.6288	50819.1719	612.4569		0
TAST-II-3,5-FY	51431.6288	51358.8477	72.7811		15
AlaDH-wt	40765.6836	40766.418	-0.7344	11	-
AlaDH-3-FY (exo.)	40963.5736	40963.4688	0.1048		11
AlaDH-3-FY	40963.5736	40962.9844	0.5892		11
AlaDH-2-FY	40963.5736	40963.0742	0.4994		11
AlaDH-2,3-FY	41161.4636	41125.2656	36.198		10
AlaDH-3,5-FY	41161.4636	41124.3477	37.1159		10

Differential scanning fluorimetry

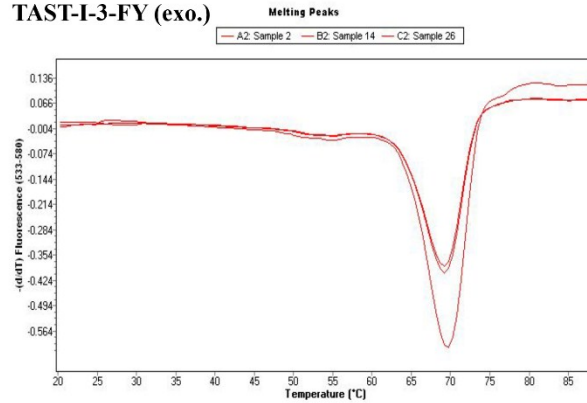
Differential scans were performed using a high-sensitivity DSC (Nano-DSC, TA Instruments, Delaware, USA). The sample and the reference cells were filled with 30 μL of protein (0.5 mg/mL) and 10 μL SYPRO orange dye (1:1000 times dilution) in 10 mM Tris-HCl buffer (pH 8.0). Calorimetric measurements were conducted in a microtitre plate at a scan rate of 1°C/min. Buffer tracings were obtained under the same conditions and subtracted from sample curves. The observed thermograms were baseline corrected and normalized data were analyzed using NanoAnalyze software.⁸

A.

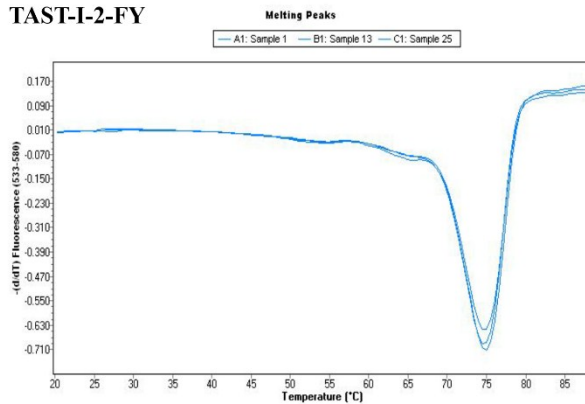
TAST-I-wt



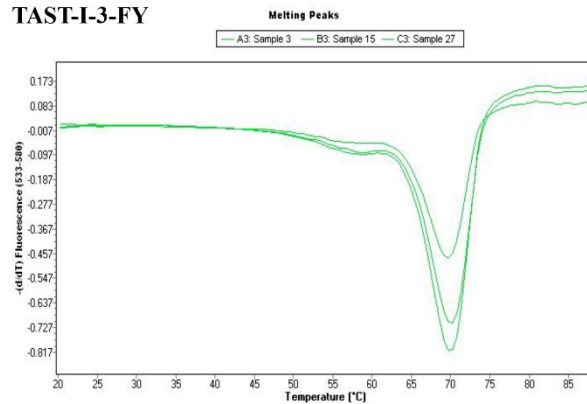
TAST-I-3-FY (exo.)



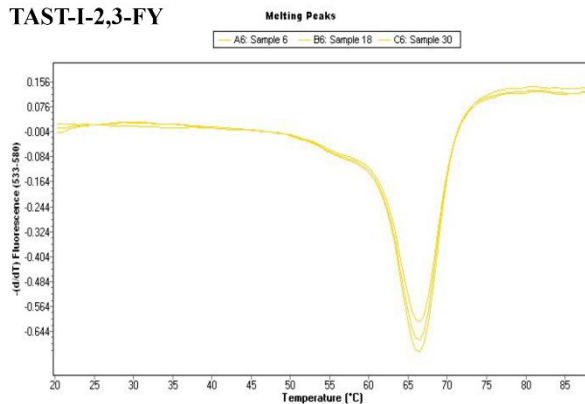
TAST-I-2-FY



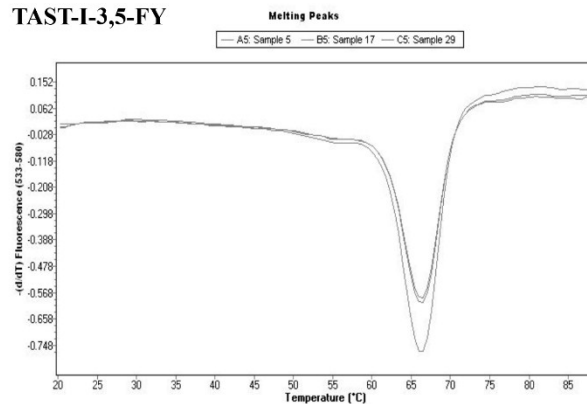
TAST-I-3-FY



TAST-I-2,3-FY

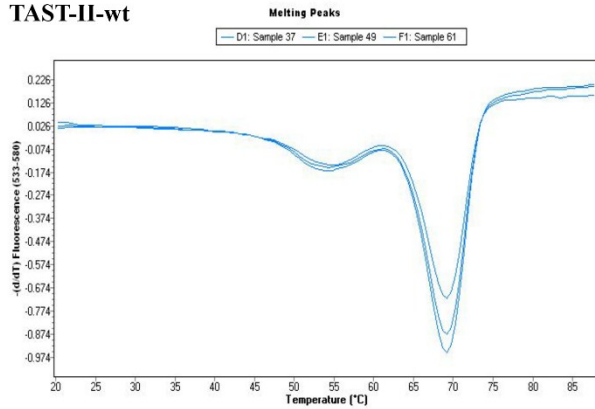


TAST-I-3,5-FY

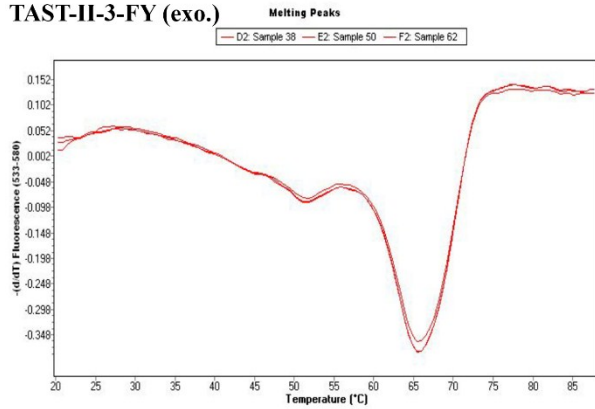


B.

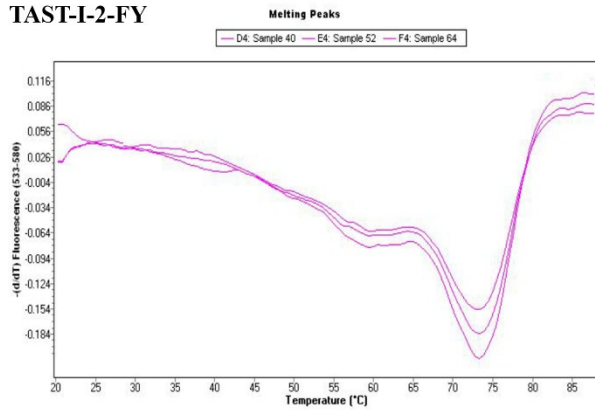
TAST-II-wt



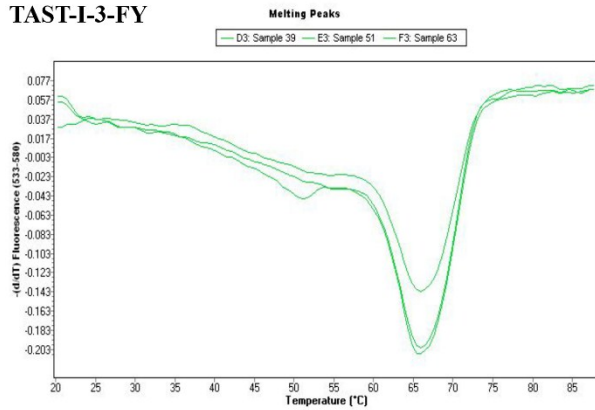
TAST-II-3-FY (exo.)



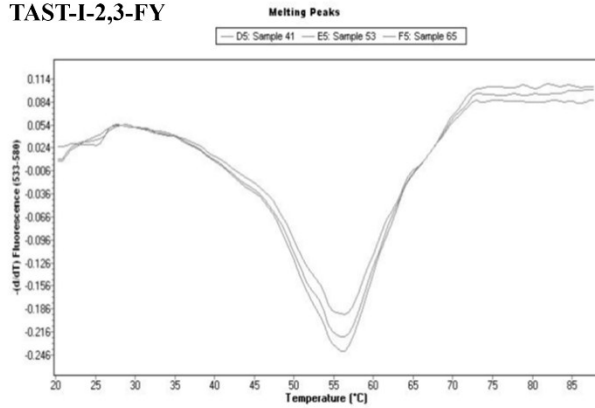
TAST-I-2-FY



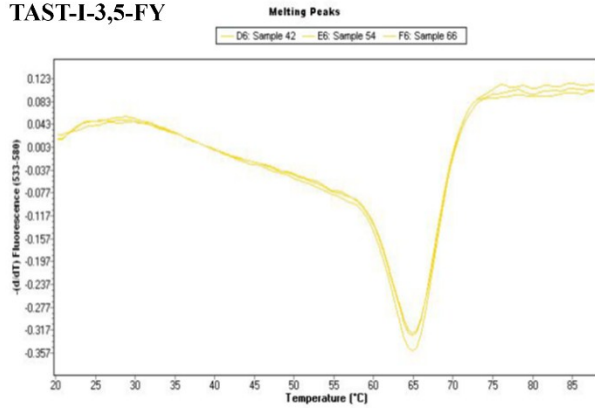
TAST-I-3-FY



TAST-I-2,3-FY



TAST-I-3,5-FY



C.

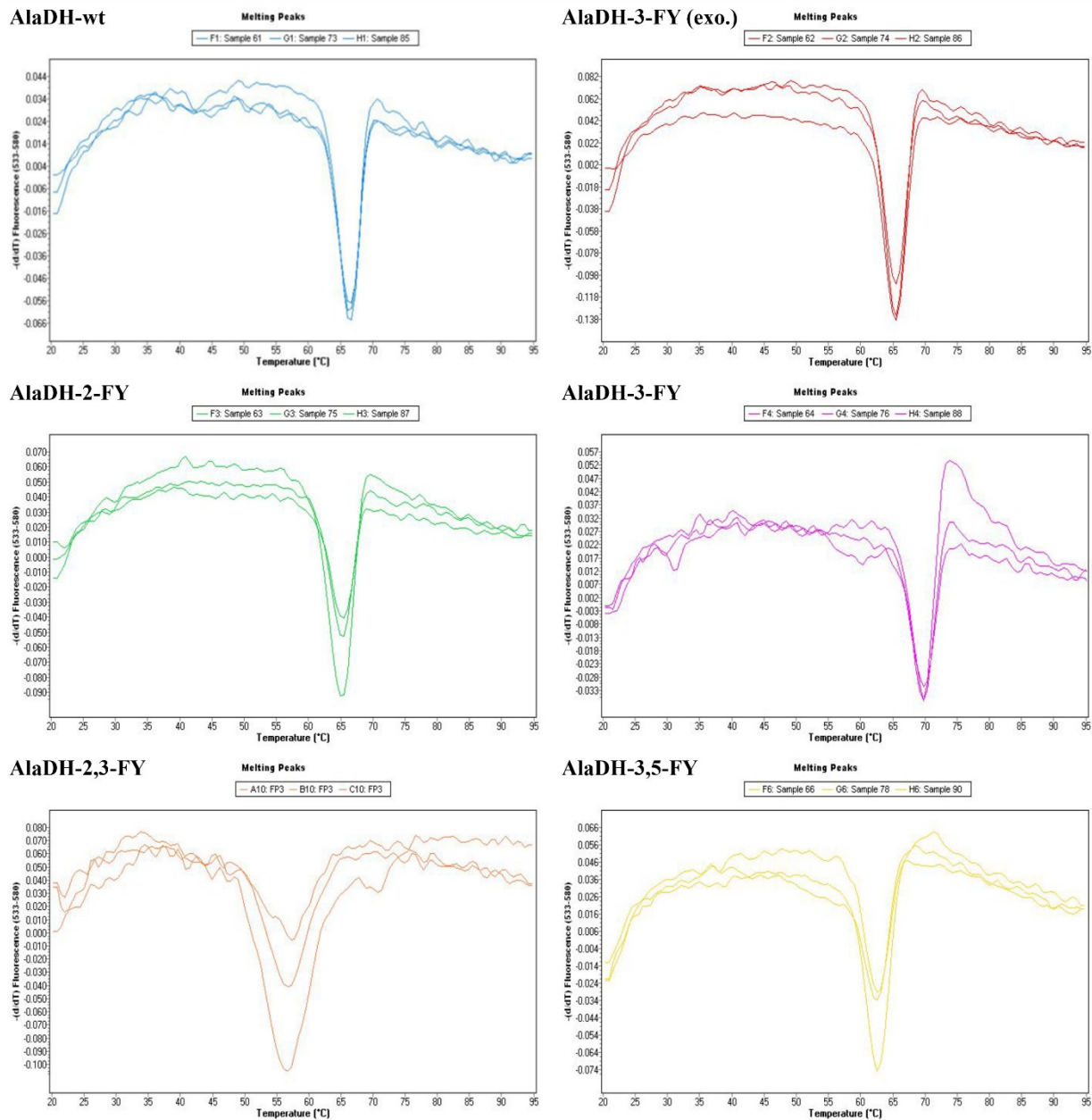


Figure S14. Differential scans of ω -TAST-I, ω -TAST-II and AlaDH wild type and their Fluorotyrosine incorporated variants to find the melting point (T_m). **A)** Fluorotyrosine derivatives incorporated into TAST-I. **B)** Fluorotyrosine derivatives incorporated into TAST-II. **C)** Fluorotyrosine derivatives incorporated into AlaDH.

Table S5. Melting temperatures of mutant enzymes.

Mutant protein	Melting temperature (°C)		
	ω-TAST-I	ω-TAST-II	AlaDH
Tyr	73.9	69.4	66.4
2-FY	77.5	73.5	70.2
3-FY	70.3	66.1	65.1
3-FY (exo.)	70.1	66.3	65.2
2,3-FY	67.0	65.0	63.5
3,5-FY	70.1	66.3	65.2

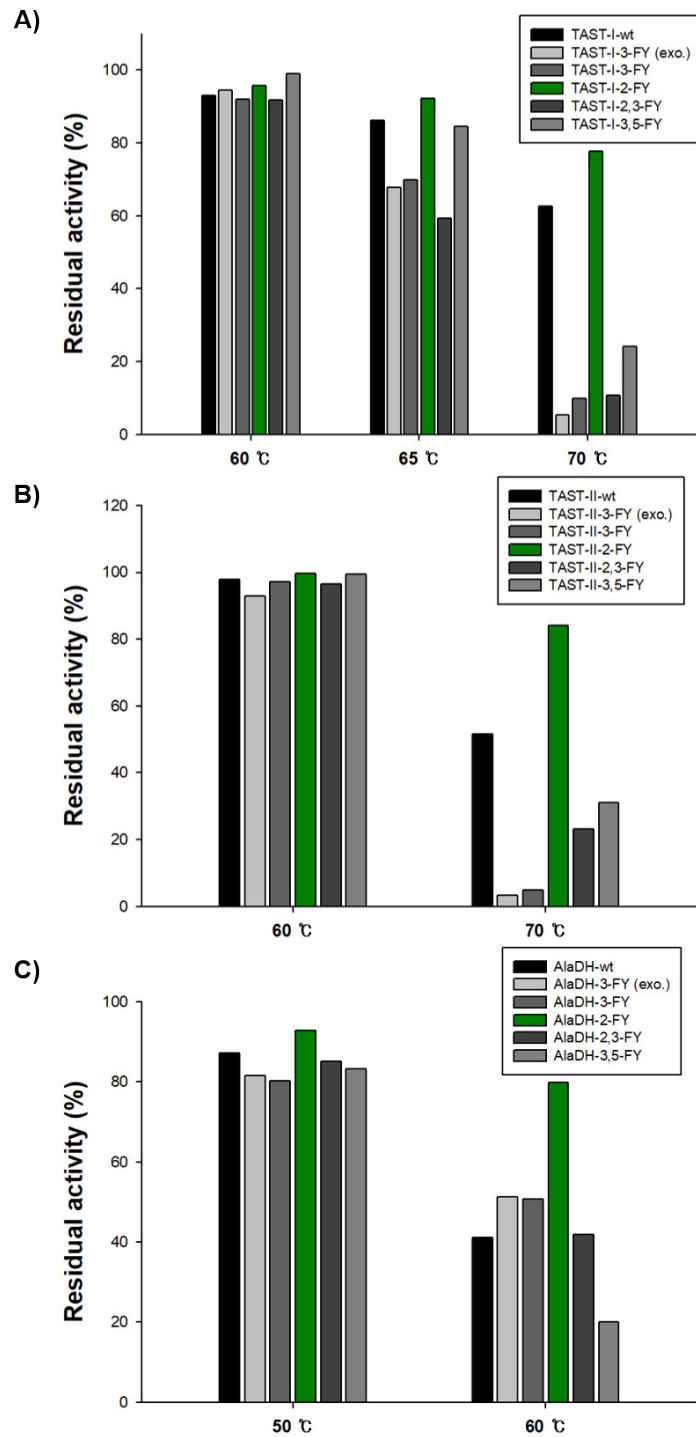


Figure S15. A) Residual activities of purified ω -TAST-I mutants incubated at different temperatures for 1 h. Enzyme reactions for each sample were carried out in a reaction volume 500 μ L containing 100 mM Tris-HCl buffer (pH 8.0), 10 mM (*S*)- α -MBA, 10 mM pyruvate and 0.1 mM PLP for 30 min at 37 °C. **B)** Residual activities of purified ω -TAST-II mutants incubated at different temperatures for 1 h and enzyme reaction for each sample were carried out in a reaction volume 500 μ L containing 100 mM Tris-HCl buffer (pH 8.0), 10 mM (*S*)- α -MBA, 10 mM pyruvate and 0.1 mM PLP for 30 min at 37 °C. **C)** Residual activity of purified AlaDH mutants incubated at different temperatures for 1 h and enzyme reaction for each sample were carried out in reaction volume 500 μ L containing 100 mM Tris-HCl buffer (pH 8.0), 10 mM alanine and 10 mM NAD⁺ for 30 min at 37 °C.

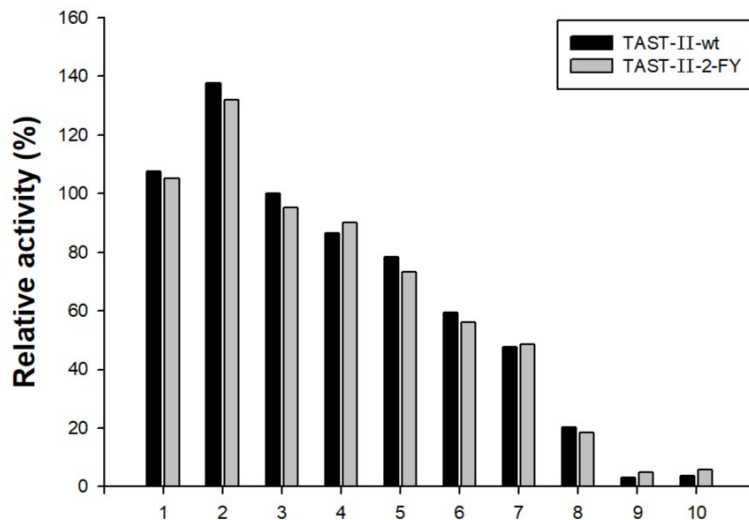


Figure S16. The activity of ω -TAST-II-2-FY, and ω -TAST-II-wt towards various amine donors tested. Reaction conditions: reaction volume of 500 μ L containing 100 mM Tris-HCl buffer (pH 8.0), 10 mM amine donor, 10 mM pyruvate, 0.1 mM PLP for 30 min at 37°C. Relative activity for amino donors was calculated by taking **3** as a model substrate.

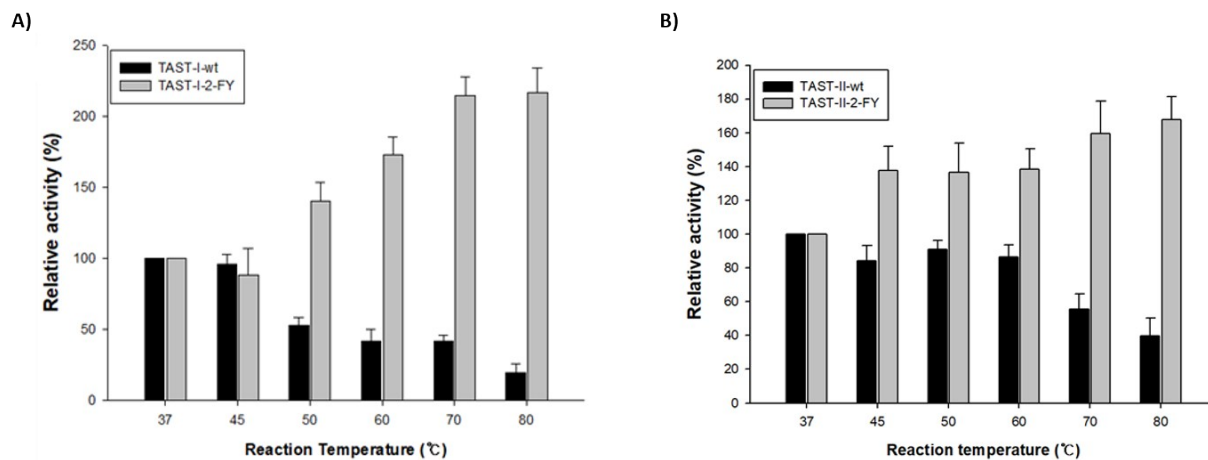


Figure S17. A) The activity of ω -TAST-I-2-FY and ω -TAST-I-wt at varying reaction temperatures. Reaction conditions; reaction volume of 500 μ L containing 100 mM Tris-HCl buffer (pH 8.0), 10 mM (S)- α -MBA, 10 mM pyruvate, 0.1 mM PLP for 30 min at different temperatures. Specific activity of TAST-I-wt at 37 °C was taken as 100%. **B)** The activity of ω -TAST-II-2-FY and ω -TAST-II-wt at varying reaction temperatures. Reaction conditions; reaction volume of 500 μ L containing 100 mM Tris-HCl buffer (pH 8.0), 10 mM (S)- α -MBA, 10 mM pyruvate, 0.1 mM PLP for 30 min at different temperatures. Specific activity of TAST-II-wt at 37 °C was taken as 100%.

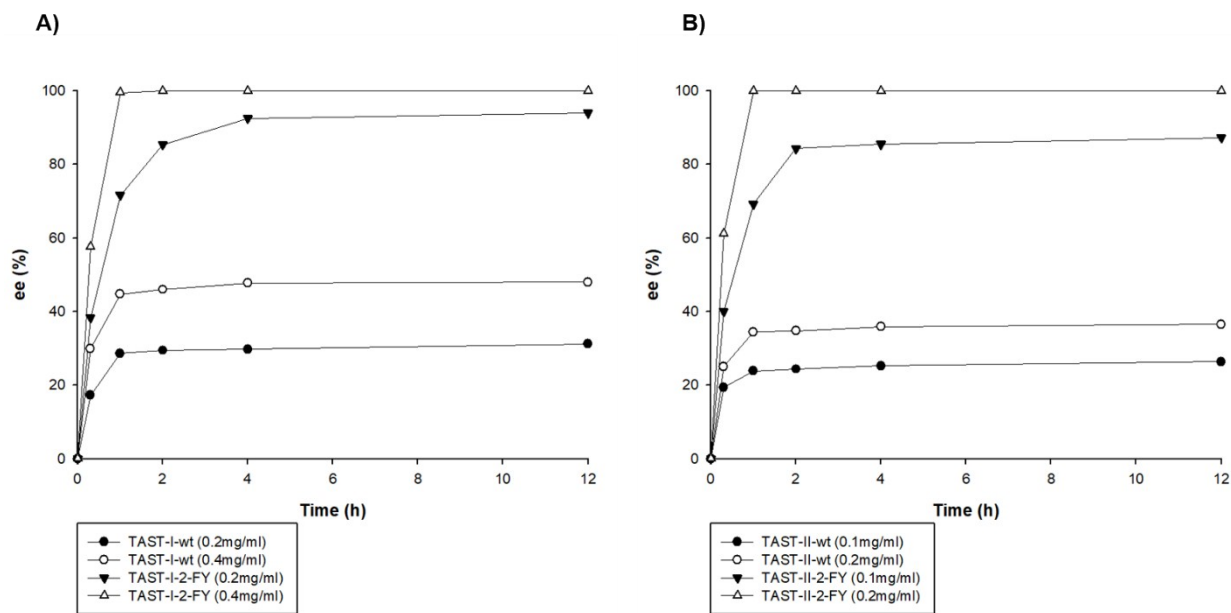


Figure S18. Reaction profiles of the kinetic resolution of *rac*- α -methylbenzylamine (*rac*- α -MBA). Reaction conditions: reaction volume of 1ml 100 mM Tris-HCl buffer (pH 8.0), 50 mM *rac*-Methylbenzylamine, 50 mM pyruvate, 0.5 mM PLP at 70 °C.

References:

1. B. Seisser, R. Zinkl, K. Gruber, F. Kaufmann, A. Hafner, W. Kroutil, *Adv. Synth. Catal.* 2010, **352**, 731-736.
2. N. Ayyadurai, N. S. Prabhu, K. Deepankumar, S. G. Lee, H. H. Jeong, C. S. Lee, H. Yun, *Angew. Chem.* 2011, **123**, 6664-6667
3. S. Mathew, S. P. Nadarajan, T. Chung, H. H. Park, H. Yun, *Enzyme Microb. Technol.*, 2016, **87**, 52-60.
4. S. Yoon, M. D. Patil, S. Sarak, H. Jeon, G-H. Kim, T.P. Khobragade, S. Sung, H. Yun, *ChemCatChem* 2019, **11**, 1898-1902.
5. W. F. Aaron, T. D. Vivian, J. K. Rebekah, C. F. Emil, Y. Yanbo, A. A. Brooke, K. Ramanarayanan, S. C. Jason, L. Lingjun, E. R. Floyd, *J. Am. Chem. Soc.* 2019 **141**, 10644-10653
6. J. K. Villa, H. A. Tran, M. Vipani, S. Gianturco, K. Bhasin, B. L. Russell, E. J. Harbron, D. D. Young, *Molecules* 2017, **22**, 1194.
7. N. Ayyadurai, N. S. Prabhu, K. Deepankumar, A. Kim, S. G. Lee, H. Yun, *Biotechnol. Lett.* 2011, **33**, 2201.
8. K. Deepankumar, S. P. Nadarajan, S. Mathew, S. G. Lee, T. H. Yoo, E. Y. Hong, B. G. Kim, H. Yun, *ChemCatChem* 2015, **7**, 417-421.